Analysis of Unresolved Spectral Infrared Signature for the Extraction of Invariant Features

Anil Chaudhary[1], Tamara Payne[1], Seth Wilhelm[1], Stephen Gregory[2], Mark A. Skinner[2], Richard Rudy[3], Ray Russell[3], James Brown[4], Phan Dao[4]

[1] Applied Optimization, [2] Boeing LTS, [3] The Aerospace Corporation,
[4] AFRL Space Vehicles Directorate, Hanscom AFB, Lexington, MA

ABSTRACT

This paper demonstrates a simple analytical technique for extraction of spectral radiance values for the solar panel and body from an unresolved spectral infrared signature of 3-axis stabilized low-earth orbit (LEO) satellites. It uses data collected by The Aerospace Corporation's Broad-band Array Spectrograph System (BASS) instrument at the Air Force Maui Optical and Supercomputing (AMOS) site. The observation conditions were such that the signatures were due to the emissive phenomenology and contribution of earthshine was negligible. The analysis is based on a two-facet orientation model of the satellite. This model captures the basic, known behavior of the satellite body and its solar panels. One facet points to nadir and the second facet tracks the sun. The facet areas are unknown. Special conditions are determined on the basis of observational geometry that allows separation of the spectral radiance values of the solar panel and body. These values remain unchanged (*i.e.*, are invariant) under steady illumination conditions even if the signature appears different from one observation to another. In addition, they provide information on the individual spectral makeup of the satellite solar panel and body materials.

1.0: INTRODUCTION

When a satellite is observed in the infrared, its signature varies with the phase angle. This is because the satellite adjusts its orientation with respect to the sun and the earth and the projected view of the satellite changes continuously with respect to the sensor. When the satellite enters or exits the shadow of the earth, its solar panel and body temperatures may change depending on the thermal control of the satellite. If a satellite is illuminated continuously and is operating under steady-state conditions, its solar panel and body reach a thermal equilibrium with its environment such that the thermal energy emitted by the solar panel and the body remain constant. Thus the signature is a function of entities that remain constant (or, are invariant) and entities that are varying. The invariant entities are the spectral radiance values (*i.e.*, the thermal energy emitted as a function of wavelength) under steady-state conditions for satellite surfaces. The variable entities are a function of the satellite position and its projected view. The present work is to capture the invariant and variable entities in a simple analytical model for the purpose of calculation of the spectral radiance values for the satellite solar panel and the body separately.

Tab1e 1 shows a list of five signatures that were analyzed in this work. The signatures are for three satellites. All satellites are three-axis stabilized LEO objects of the same type. The basic premise in the analysis is that since these satellites are of the same type, the spectral radiance values for the solar panel and body should be the 'same' for all satellites even though their signatures may look different. This is an extension of the basis in Reference 5. The data was collected at AMOS by the 3.6 meter telescope using the BASS instrument. The original data is in over a hundred bands. The data was binned into four wavebands for this analysis (Table 2). The wavebands match roughly with the atmospheric windows. However, no special effort was undertaken in order to optimize the wavebands. Within the four wavebands, BASS-A waveband is more susceptible to the scattered/reflected solar flux as compared to the other wavebands.

The five signatures are shown in Figures 1a to 1e. The signatures are normalized by the square of the satellite range. The data is shown as a semi-log plot of average brightness in each waveband versus the phase angle. The units of brightness data are log(Watts/square meter-micron). The signature brightness is generally consistent for all five signatures, but the shape and character of the signatures are different. The goal of this paper is to solve for the intrinsic commonality between these signatures.

Table 1: List of the Signatures Analyzed

Satellite	Observation ID
A	39-080916-1435
B	86-080916-1401
B	86-080920-1503
B	86-080923-1330
C	93-080920-1432

Table 2: Definition of Binning Wavebands

Waveband ID	Range
BASS-A	3.7 to 4.0 micron
BASS-B	4.8 to 5.0 micron
BASS-C	8.2 to 9.3 micron
BASS-D	9.9 to 13 micron

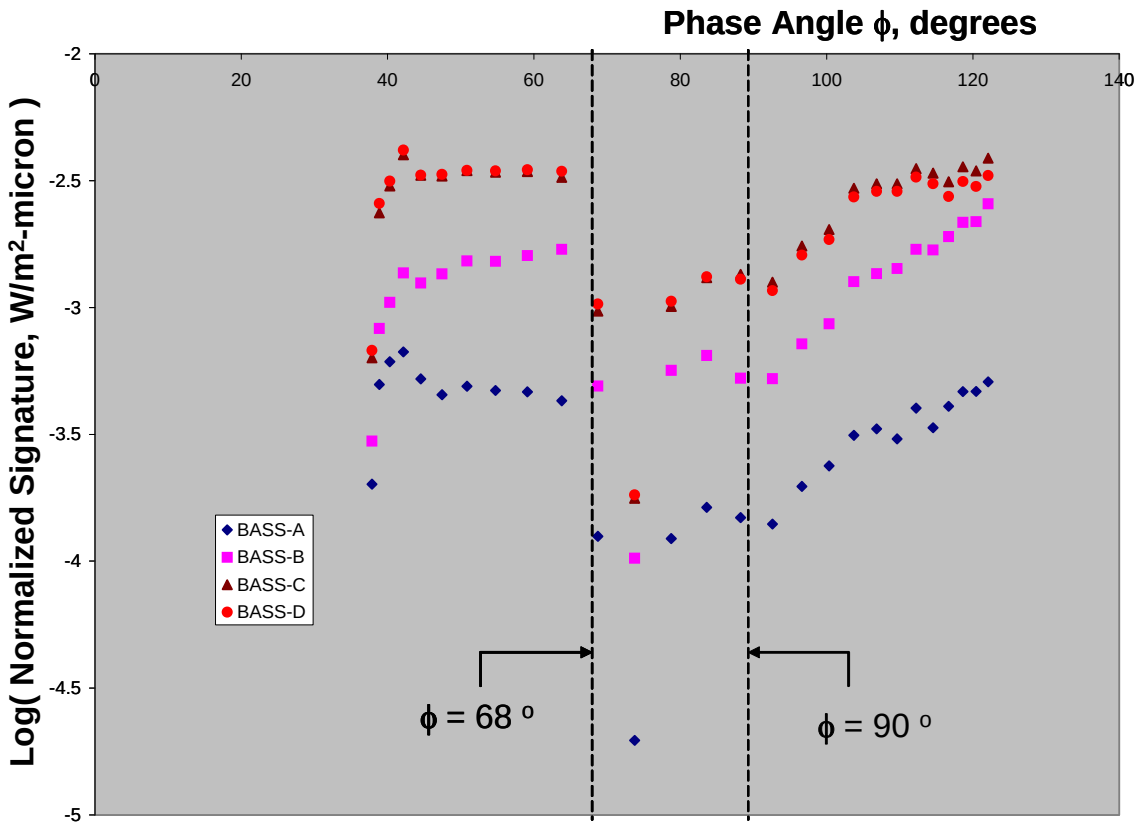

Figure 1a: Range Normalized Signature for Satellite-A (Observation ID: 39-080916-1435)

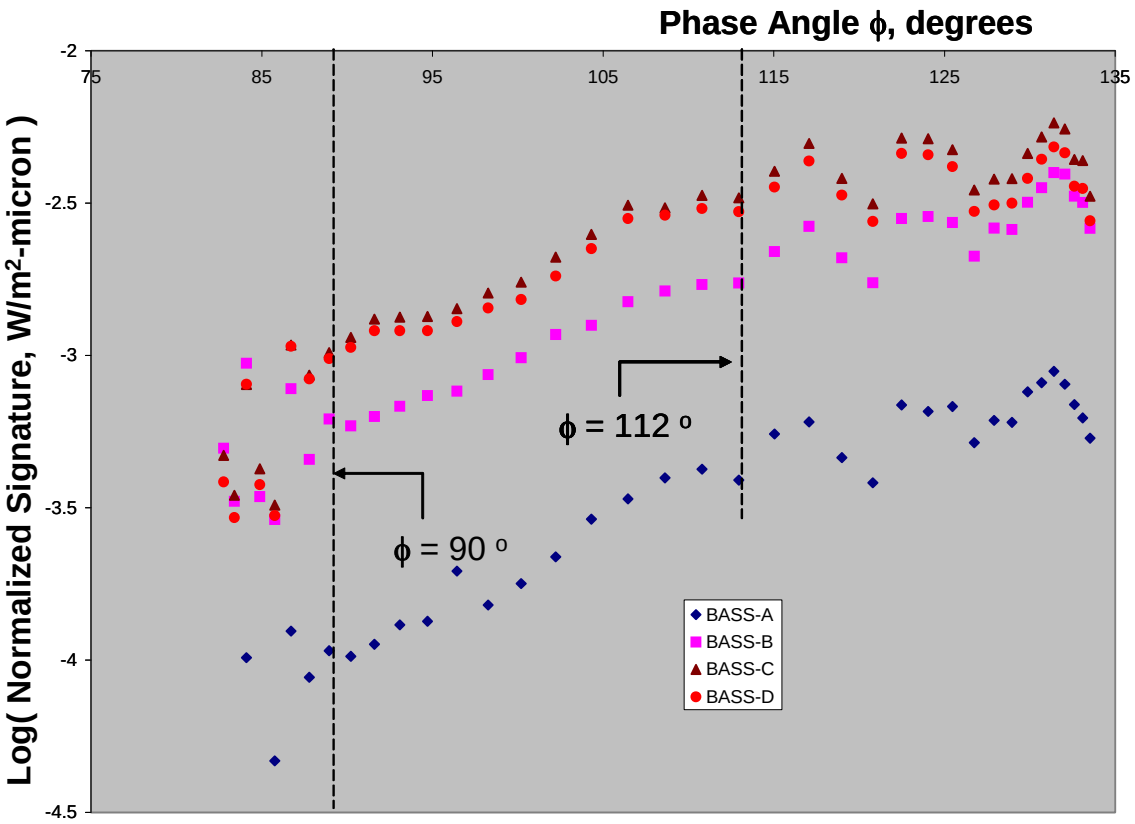

Figure 1b: Range Normalized Signature for Satellite-B (Observation ID: 86-080916-1401)

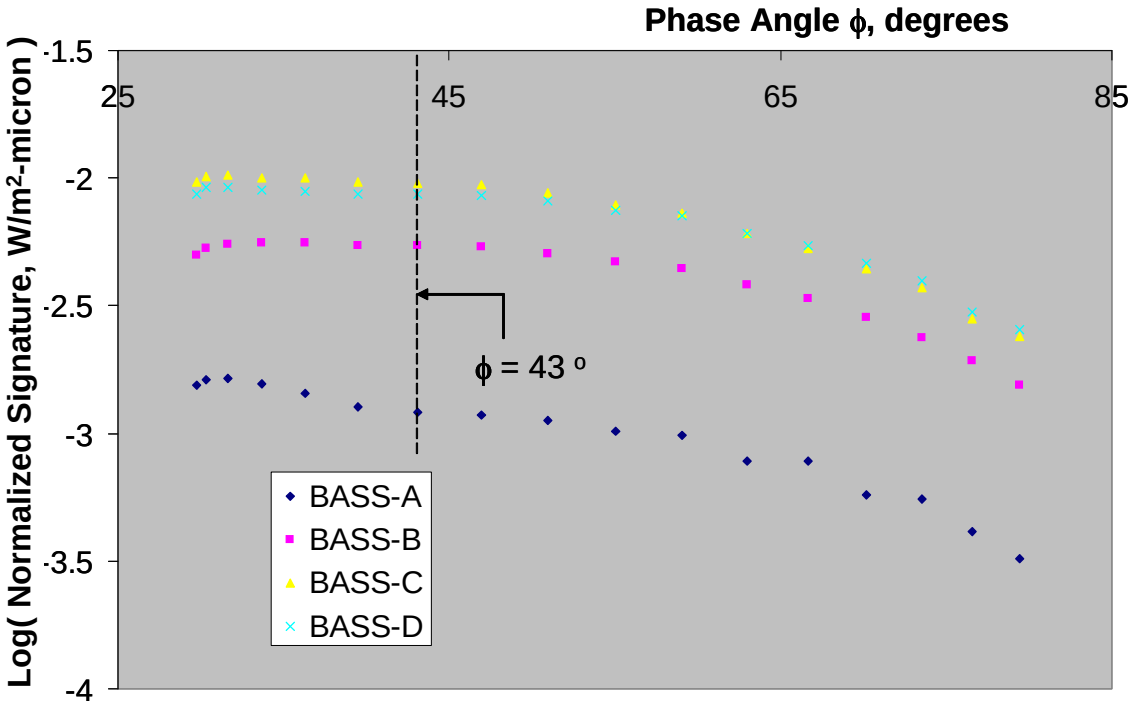

Figure 1c: Range Normalized Signature for Satellite-B (Observation ID: 86-080920-1503)

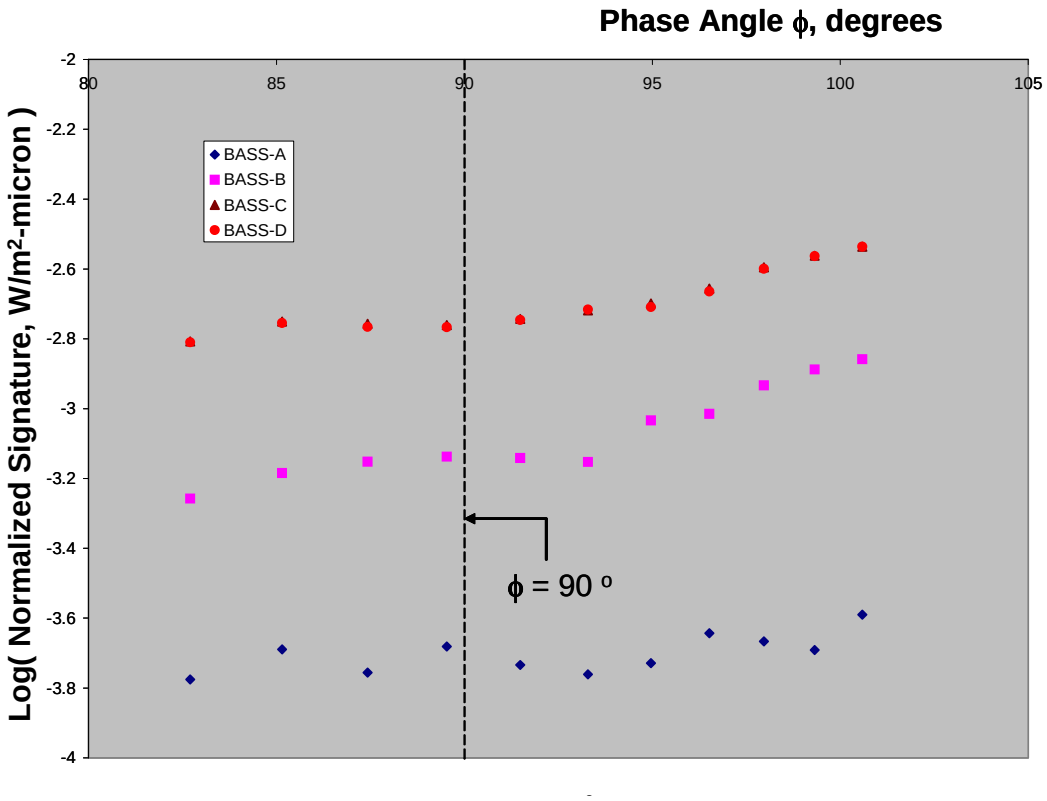

Figure 1d: Range Normalized Signature for Satellite-B (Observation ID: 86-080923-1330)

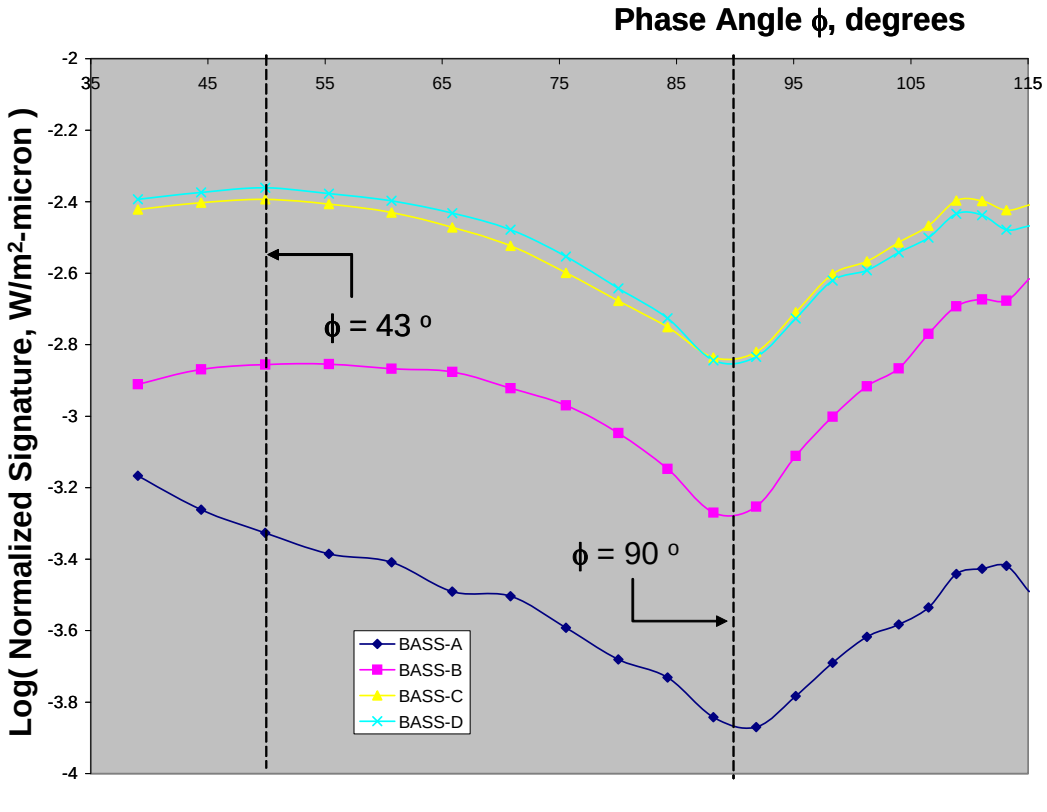

Figure 1e: Range Normalized Signature for Satellite-C (Observation ID: 93-080920-1432)

2.0: SPACECRAFT OBSERVATION GEOMETRY AND ITS TWO-FACET ORIENTATION MODEL

This work is based on two assumptions, namely; (1) the orbital elements for the three-axis stabilized satellites are known, and (2) the dimensions and temperatures for the solar panel and body are unknown. The first assumption means that we know the orientation of the satellite components. The second assumption means that the spectral radiance (*i.e.*, the product of the intensity of emitted thermal flux as per Planck's law multiplied by the area) for the solar panel and the body are unknown. The observed signature is an unknown mixture of the two spectral radiance values.

Figure 2 shows a schematic of the spacecraft observation geometry. It is defined in terms of four coordinates and three angles. The coordinates are for the sun, spacecraft, sensor and the earth. The sensor is assumed to be ground-based. The angles are: (1) The sun-spacecraft-sensor angle or the phase angle, ϕ; (2) The sensor-spacecraft-nadir angle, which is denoted as η and called as the nadir angle in this paper; (3) Third is the sun-spacecraft-earth (or, the sun-spacecraft-nadir) angle, which is denoted as ψ.

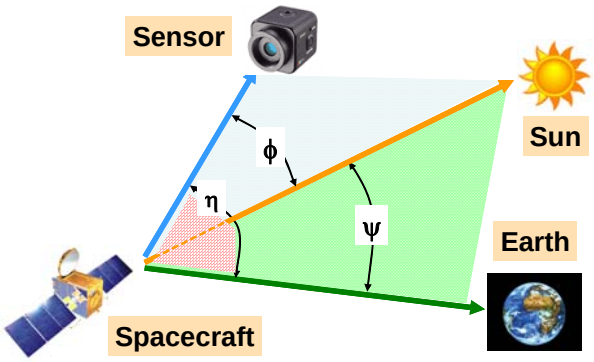

Figure 2: The Spacecraft Observation Geometry

The two-facet orientation model for the satellite idealizes the solar panel as one planar facet that always points to the sun and a second planar facet that points to nadir (Figure 3a). The thermal emission from both facets is assumed to follow Lambert's cosine law. The solar panel facet is denoted as the P-facet and the body facet is denoted as the B-facet. If the size of the solar panels were known, the area of the P-facet would equal the total area of the solar panels. Figure 3b shows a 2D schematic of the model, which is useful for getting a physical insight and performing back-of-the-envelope checks. The P-facet is shown as a blue line and the B-facet is shown as an orange line. The geometry shown can occur if the sun, earth, sensor and the spacecraft were to lie in a single imaginary plane. This can occur, but the basic purpose for the figure is to illustrate the relationship between the three angles.

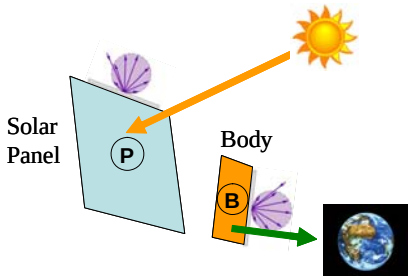

Figure 3a: Two-Facet Orientation Model

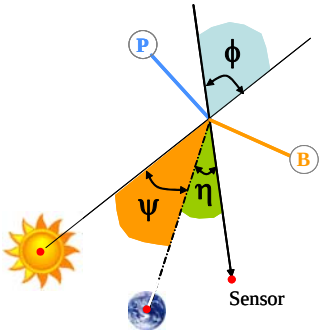

Figure 3b: A 2D-Schematic of the Two-Facet Orientation Model

Figure 4 shows the analytical expression for the infrared signature. The signature is normalized by the square of the range. The unknown value of the spectral radiance of the P-facet is denoted as P. The contribution of the P-facet to the signature equals the product of its spectral radiance (P) and the cosine of the phase angle. Similarly, for the B-facet, the spectral radiance is denoted as B. The contribution of the B-facet to the signature is similarly equal to B times the cosine of the nadir angle. The resulting analytical expression for the signature has two unknowns (namely P and B) and two known values (cosines of the phase and nadir angles). Thus, if the signature is available at two discrete time points, it is feasible to solve for the unknown values of P and B under steady-state operational conditions.

2.1: MEASURE OF ERROR IN THE USE OF TWO-FACET ORIENTATION MODEL

It is useful to critique the assumptions present in the analytical equation for the observed signature. Using a single planar facet to represent a solar panel is deemed reasonable because the solar panels are generally planar for most 3-axis stabilized satellites. The body, however, is a solid object and its representation as a single planar facet is an approximation. It is reasonable in the limit as the nadir angle tends to zero. This occurs when the spacecraft range tends to infinity. Or, the error is at least inversely proportional to the range. A quantitative measure of the error may be obtained analytically. For this purpose, we may assume that the spacecraft body is a cube. We also assume that the spectral radiances of all faces of the cube are same.

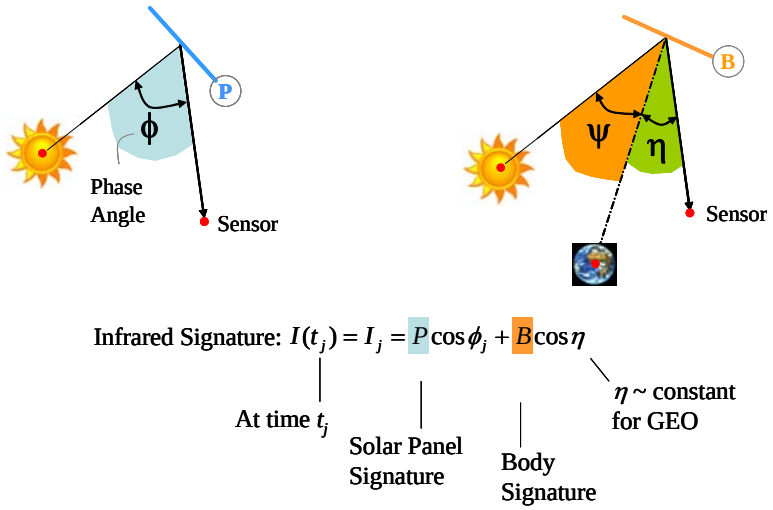

Figure 4: Analytical Expression for the Range-normalized Infrared Signature using the Two-facet Model

A cube has six faces. At least three faces of the cube are always occluded from the sensor. From the remaining three, one face points to nadir and the other two are side faces. If the two-facet idealization were exact, the contribution of the side face would be zero at all times.

Assume that only one of the side faces is visible to the sensor and the other is occluded. Then, the projected area of the visible side face would be equal to the product of its area and the cosine of the complement of the nadir angle (*i.e.*, area multiplied by $\cos(90-\eta)^o$). The B-term in the analytical expression for the infrared signature of the two-facet model may change in value by a factor equal to $\cos(90-\eta)^o$ over the duration of observation. In other words, the value of $\cos(90-\eta)^o$ is a measure of error.

For a GEO spacecraft, the nadir angle is $< 8^o$ and it is essentially constant. Or, up to 14% of the side face area may be visible to the sensor (i.e. $\cos 82^o$). Or an estimate of error bound for the body radiance is 14%.

For a MEO spacecraft (MEO), the nadir angle can vary from -15^o to $+15^o$ over a period of several hours. The rate of change of nadir angle is $< 0.10^o$ per minute. Up to 25% of the side face may become visible to the sensor at low values of elevation. The resulting estimate of error bound for the body radiance is 25%.

For most observations of LEO spacecraft (LEO), the nadir angle would be within -70^o to $+70^o$. The estimated error bound for the body radiance is 93%. This is large, which is a reason for the use of special observation conditions that can circumvent this error.

3.0: USE OF THE TWO-FACET ORIENTATION MODEL

Method 1: Use of Range and Nadir Angle Normalized Signature

The range-normalized infrared (emissive) signature for the two facet orientation model is given by:

$$I(t_j) = I_j = P\cos\phi_j + B\cos\eta_j \qquad \text{Equation (1)}$$

For single band data, Equation (1) is a scalar equation. For a multi-spectral or hyperspectral signature, Equation (1) is a vector equation, where each row is the signature for one waveband. The cosine terms are common for all wavebands and they account for the orientation of the satellite. The subscript '*j*' denotes the signature and cosine terms at an instant of time, t_j.

The range and cos(nadir angle) normalized signature is given by:

$$\frac{I(t_j)}{\cos\eta_j} = P\frac{\cos\phi_j}{\cos\eta_j} + B \qquad \text{Equation (2)}$$

When the phase angle equals 90°, the contribution of the solar panel drops out. *Thus the spectral radiance of the body is equal to the range and cos(nadir angle) normalized signature when the phase angle is 90°.*

Method 2: Stationarity of the Nadir Angle with respect to the Phase Angle

The derivative of a range normalized signature with respect to the cosine (phase angle) is given as follows.

$$\left(\frac{dI_j}{d\cos\phi_j}\right) = P + B\frac{\sin\eta_j}{\sin\phi_j}\frac{d\eta_j}{d\phi_j} \qquad \text{Equation (3)}$$

When $d\eta/d\phi$ equals zero, the right hand side of Equation (3) contains no contribution from the body. The only remaining term is the solar panel spectral radiance, P. *Thus the spectral radiance of the solar panel is equal to the derivative of the range normalized signature with respect to the cosine of the phase angle when the derivative $d\eta/d\phi$ is equal to zero.*

In order to determine the solar panel spectral radiance, it is convenient to search for instants of time during the observation period when $d\eta/d\phi$ is equal to zero. This is readily performed using the orbital elements data for the satellite and it has been found to occur routinely in LEO satellites. For GEO objects, $d\eta/d\phi$ is nominally close to 'zero' at all times.

Equation (3) also provides an interesting corollary. Assume that the body is a cube and that it has no articulating components. Then, the contribution of the side face to the signature is proportional to $\cos(90-\eta)$ (see Section 2.1). When $d\eta/d\phi$ is equal to zero, $d(90-\eta)/d\phi$ is also equal to zero (as per the chain rule in calculus). Thus, even if the two facet approach were enhanced to include the side faces, their contribution will drop out at the same time when $d\eta/d\phi$ is equal to zero.

Benefit of the Two Methods: It is a common practice today to utilize the observed signature as is in order to determine the brightness temperature, distribution temperature, and/or the color temperature. Since the observed signature is a mixture of contributions from the solar panel and the body, the computed temperature is a weighted value of solar panel and body temperatures. Indeed, the computed value for the temperatures can change with the phase angle even if the spacecraft was in a steady-state operation and illumination. This is not physical. For example, assume that a satellite was observed simultaneously by sensors located at different sites. The projected view of the satellite would be different at each site, depending on its location. The observed signature would contain contributions from the solar panel and the body that would differ from site to site. Consequently, if these signatures were analyzed, the computed value of temperature would be different from site to site as well.

A salient benefit of this work is that it shows a way for separating the spectral radiances of the solar panel and the body from the observed signature. This is also known as "unmixing", and there are many algorithms for unmixing in the literature. These algorithms need to solve a rectangular system of equations because the number of independent equations exceeds the number of unknowns. This creates questions on the uniqueness of the answer. The present work provides a simple, analytical method for unmixing.

4.0: PROCESSING OF LEO OBSERVATIONS DATA

Nadir Angle vs. Phase Angle Plots:

Orbital calculations were performed for each observation in order to compute the phase angle and nadir angle values at each instant of time. This data is shown in Figure 5. The locations where $d\eta/d\phi$ is equal to zero are marked with red dots. These graphs identify the special conditions listed in Table 3, which are given as per Equations (2) and (3) in Section 3.0.

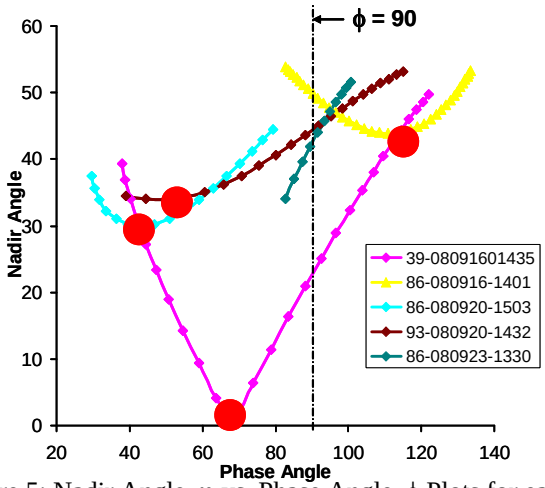

Figure 5: Nadir Angle, η vs. Phase Angle, ϕ Plots for each Observation
Note that the location where $d\eta/d\phi$ is equal to zero is marked with a red dot.

Table 3: Special Conditions Available among the Observations

Satellite	Observation ID	Special Conditions Available
A	39-080916-1435	$\phi = 90^o$, $d\eta/d\phi = 0$ at $\phi = 68^o$
B	86-080916-1401	$\phi = 90^o$, $d\eta/d\phi = 0$ at $\phi = 112^o$
B	86-080920-1503	$d\eta/d\phi = 0$ at $\phi = 43^o$
B	86-080923-1330	$\phi = 90^o$
C	93-080920-1432	$\phi = 90^o$, $d\eta/d\phi = 0$ at $\phi = 49^o$

Use of Method 1 for the Calculation of Body Spectral Radiance

Figure 1 shows the plots of range and nadir angle normalized signature versus phase angle for four signatures where the condition that $\phi = 90^o$ is available. As per Equation 2, this normalized signature equals the body radiance when $\phi = 90^o$. Table 4a shows the body spectral radiance values for satellites A, B and C. Two observations are processed for satellite B. The body spectral radiance values extracted from the four different observations are consistent with each other even though the individual signatures have distinctly different appearances. This consistency of the spectral radiance values is because satellites A, B and C belong to the same family. The computed spectral radiance is useful for the calculation of the body temperature for satellites A, B and C.

Use of Method 2 for the Calculation of Solar Panel Spectral Radiance

Attempts to determine the solar panel spectral radiance using the derivative form shown in Equation (4) were more challenging due to the use of a derivative. It is, however, useful to note that the processed signatures were collected with no special planning as regards to the condition $d\eta/d\phi = 0$. The method uses only the available information. This may be improved with advance planning of the observations.

The orbital calculations detected four special locations when $d\eta/d\phi = 0$ (Figure 5). These special locations

are also shown in Figure 1. It is interesting to see that there is a change in signature shape at this special location in Figures 1a and 1b. The general trend or derivative in these figures is that the brightness is increasing with the cosine of the phase angle. In other words, the left hand side of Equation (3) is positive, which is a requirement because the spectral radiance cannot be negative. Table 4b shows the solar panel spectral radiance values that were computed from these two signatures. These radiance values are deemed useful for calculation of the solar panel temperature.

The general trend in Figure 1c at the special location is almost flat. Thus Equation (3) prediction is a small, but positive, value for the P-facet spectral radiance. The trend in Figure 1e is also flat for two wavebands, decreasing for one waveband and increasing for one waveband. This would provide an unphysical result. The analysis of these two signatures needs further work.

Table 4a: Log of the Mean Spectral Radiance for the Body
[the values are $\log_{10}$(flux in W/m^2-micron)]

Satellite	Observation ID	BASS-A	BASS-B	BASS-C	BASS-D
A	39-080916-1435	-3.75	-3.25	-2.75	-2.75
B	86-080916-1401	-3.75	-3.0	-2.75	-2.75
B	86-080923-1330	-3.60	-3.0	-2.70	-2.70
C	93-080920-1432	-3.75	-3.25	-2.75	-2.75

Table 4b:Log of the Mean Spectral Radiance for the Solar Panel
[the values are $\log_{10}$(flux in W/m^2-micron)]

Satellite	Observation ID	BASS-A	BASS-B	BASS-C	BASS-D
A	39-080916-1435	-3.1	-2.5	-2.2	-2.2
B	86-080916-1401	-3.0	-2.4	-2.1	-2.1

Comparing the spectral radiance of the body and the solar panel, it is observed that the body spectral radiance is smaller. The spectral radiance of the solar panel is roughly four times as large as the body. This ratio is higher is the BASS-A waveband as compared to the other three, higher-wavelength wavebands. This difference may be potentially attributed to the scattered/reflected solar flux in BASS-A waveband. The shapes of the B- and P-facet spectral radiances are similar in wavebands BASS-B, BASS-C and BASS-D. We may infer from this similarity that the body and solar panel temperatures are also similar to each other and that the solar panel is significantly larger than the body. If the emissivity of the solar panel and the body were similar, the solar panel would be roughly four times as large as the body.

5.0: BENEFITS OF THE REPORTED WORK

There are three benefits we see with this approach:

1) This work demonstrates a simple, analytical method for isolating the spectral radiances of the solar panel and body for three-axis stabilized spacecraft in LEO, MEO and GEO.
2) The isolated spectral radiance values comprise intrinsic, invariant knowledge that is useful for the determination of solar panel and body temperature individually.
3) The analytical methods are useful for the processing of single band radiometric data as well as multi-spectral and hyperspectral data.

This paper also presents an analytical estimate of the measure of error due to the idealization of the geometry by a two-facet orientation model. This error is inversely proportional to the satellite range. The reported results are deemed valid on the basis that the computed values of P and B are invariant even though they are extracted from signatures that look different from each other. In this sense, the method is successful in extracting the common denominator information from the signatures.

6.0: ACKNOWLEDGEMENT

Anil Chaudhary, Tamara Payne and Seth Wilhelm of Applied Optimization, and Mark Skinner of Boeing LTS gratefully acknowledge the support for this research by the AFRL/Space Vehicles Directorate. The work at Applied Optimization was supported by an SBIR Phase II Contract FA8718-08-C-0019 [References 1-3]. The present paper is based on the data from the Maui Space Surveillance System, which is operated by Detachment 15 of the US Air Force Research Laboratory's Directed Energy Directorate. The support for Richard Rudy and Ray Russell was from the The Aerospace Corporation Independent Research & Development program [Reference 4].

7.0: REFERENCES

1. Chaudhary, A., Payne, T., “Unresolved RSO Fingerprinting Using Time-Frequency Analysis”, Annual Report for the present Phase II SBIR Project, May 2009
2. Payne, T., Chaudhary, A., Gregory, S., Brown, J., Nosek, M., “Signature Intensity Derivative and its Application to Resident Space Object Typing”, AMOS 2009
3. Chaudhary, A., Payne, T., Gregory, S., and Brown, J., “RSO Fingerprinting using Non-Resolved Multi-Spectral Signatures”, SSA Meeting at AMOS 2009
4. Skinner, M.A., Gutierrez, D.J., Kim, D.L., Russell, R.W., Rudy, R.J., Gregory, S., Crawford, K., "Time-Resolved Infrared Spectrophotometric Observations of IRIDIUM satellites and related Resident Space Objects", IAC-09-A6.1.17, International Astronomical Congress 60th meeting, 12-16 October 2009, Daejeon, Republic of Korea.
5. Jorgensen, K., “Using Reflectance Spectroscopy to Determine Material Type of Orbital Debris”, Ph.D. Thesis, University of Colorado, Boulder, May 2000.